Electronic Supplementary Material (ESI) for Journal of Materials Chemistry B.


# Application of Singlet Oxygen-Activatable Nanocarriers to Boost X-ray-Induced Photodynamic Therapy and Cascaded Ferroptosis for Breast Cancer

Beibei Zhang[a, b, c, *], Hao Liu[a, b, c], Yifei Wang[a, b, c], Yong Zhang[a, b, c, *], Jingliang Cheng[a, b, c, *]

[a] Department of Magnetic Resonance Imaging, the First Affiliated Hospital of Zhengzhou University, Zhengzhou 450002, P.R. China

[b] Key Laboratory for functional magnetic resonance imaging and molecular imaging of Henan Province, Zhengzhou 450002, P.R. China

[c] Engineering Research Center of medical imaging intelligent diagnosis and treatment of Henan Province, Zhengzhou 450002, P.R. China

E-mail: zhangb0420@126.com (B. Zhang); zzuzhangyong2013@163.com (Y. Zhang); fccchengjl@zzu.edu.cn (J. Cheng)

## Experimental methods

### Materials

RPMI 1640 medium, fetal bovine serum (FBS) and trypsin were purchased from Gibco BRL (Gaithersberg, MD; USA). Cell counting kit-8 (CCK-8) and 4',6-diamidino-2-phenylindole (DAPI) were purchased from Beyotime Biotechnology Co., Ltd. (Nantong; China). Liperfluo was obtained from Beijing Dojindo Biotechnology Co., Ltd (Beijing, China). Annexin V-FITC/PI was purchased from Invitrogen Corporation (IVGN; USA). All other solvents were of analytical grade.

### Characterization

The proton nuclear magnetic resonance ($^1$H NMR) spectra were recorded in $CD_3SOCD_3$ on a 400-MHz spectrometer (Avance III, Bruker, Germany). The mean particle size, polydispersity, and zeta potential were measured by dynamic light scattering (DLS) with a Malvern Zetasizer (Nano-ZS, Malvern Instruments, UK). The morphology of nanoparticles was observed by transmission electron microscopy (TEM, Hitachi HT7700). The UV/Vis absorptions of nanoparticles and drug loading efficiency were detected on a UV/Vis spectrophotometer (UV-3600 Shimadzu, Japan). The fluorescence of SOSG was measured using a Hitachi F7000 fluorescence spectrophotometer. *In vivo* imaging of small animals was captured by Xenogen IVIS Lumina system (AMI-934M, USA). *In vivo* imaging of small animals was captured by Xenogen IVIS Lumina system (AMI-934M, USA).

### Cellular internalization of nanocarriers *in vitro*

For confocal laser scanning microscope (CLSM) observations, 4T1 cells were

seeded onto 14-mm coverslips at a density of $2 \times 10^4$ cells per well in 1.0 mL of 1640 medium, and cultured at 37 °C with 5% $CO_2$ for 12 h. The cells were then incubated with $NP_{VR}$ or D-$NP_{VR}$ for 2, 4 or 6 h, washed with PBS, fixed with 4% paraformaldehyde, and then stained with phalloidin and 4′,6-diamidino-2-phenylindole (DAPI) sequentially according to the manufacturer's protocol. The cellular internalization was then visualized on a Zeiss LSM 810 confocal microscope.

**Biosafety Evaluation**

Twenty healthy BALB/c mice were randomly divided into four groups and received *i.v.* injection daily for three times with PBS, free VP + RLS3, $NP_{VR}$, or D-$NP_{VR}$, respectively. The orbital plexus blood sampling was collected on day 7 for routine blood count, creatinine, urea nitrogen, alanine aminotransferase, and aspartate aminotransferase detection.

**Statistical Analysis**

Statistical significance was analyzed using a t-test. One-way analysis of variance (ANOVA) was used for comparisons between more than two groups. Unless specially noted, data are shown as mean ± SD ($p<0.05$).

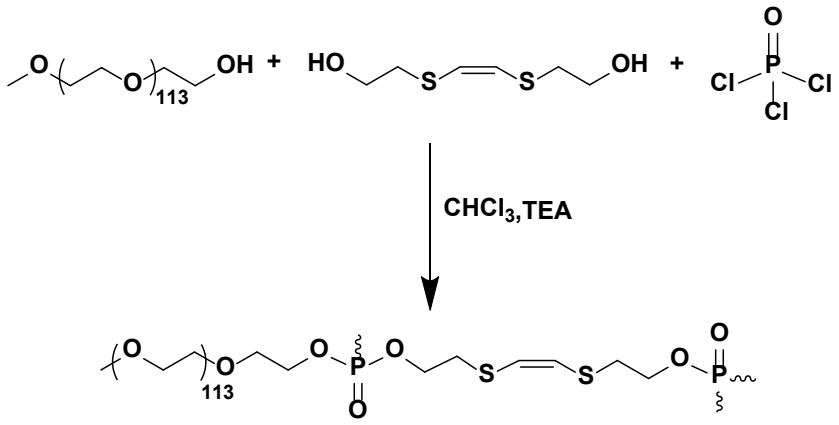


**Figure S1.** Synthetic route of 1,2-bis(2-hydroxyethylthio)ethylene bridged D-HPE.

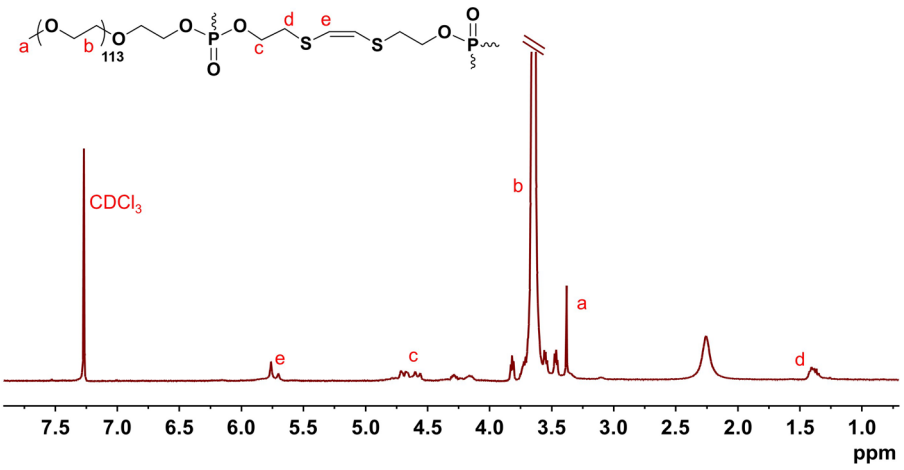


**Figure S2.** $^{1}$H NMR spectrum of D-HPE in $CDCl_3$ recorded on an AVANCE III 400 MHz spectrometer at 25 °C.

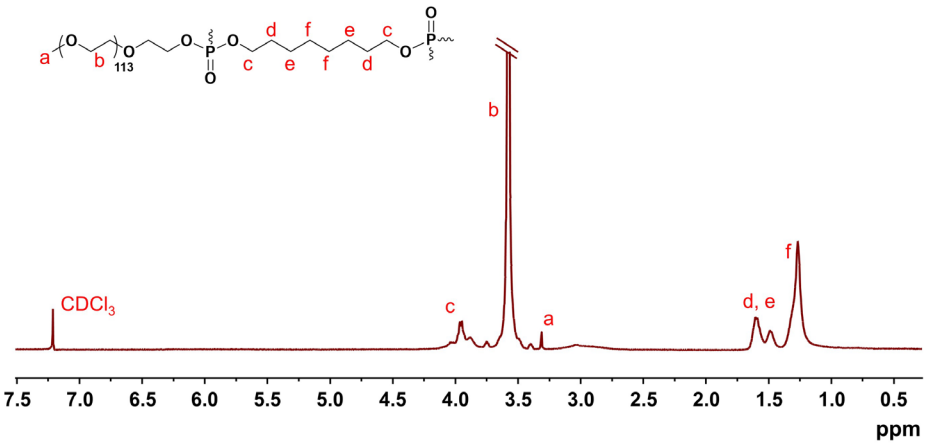


**Figure S3.** $^{1}$H NMR spectrum of HPE in $CDCl_3$ recorded on an AVANCE III 400 MHz spectrometer at 25 °C.

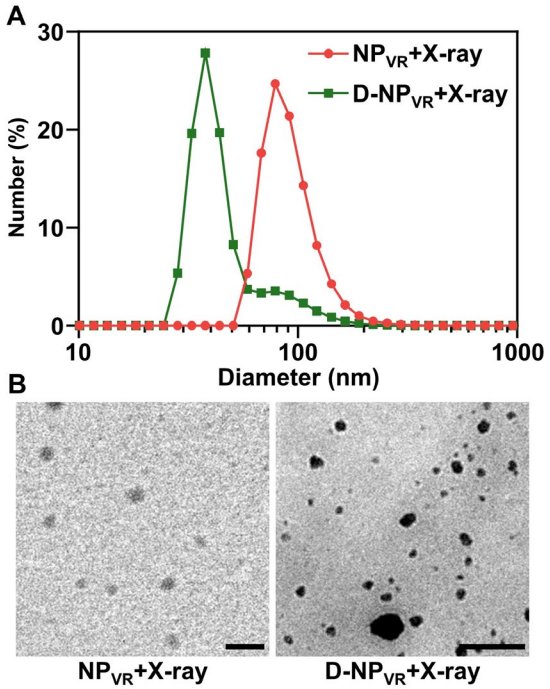


**Figure S4.** The diameter (A) and morphology (B) change of $NP_{VR}$ and D-$NP_{VR}$ with X-ray irradiation. The scale bar is 200 nm.

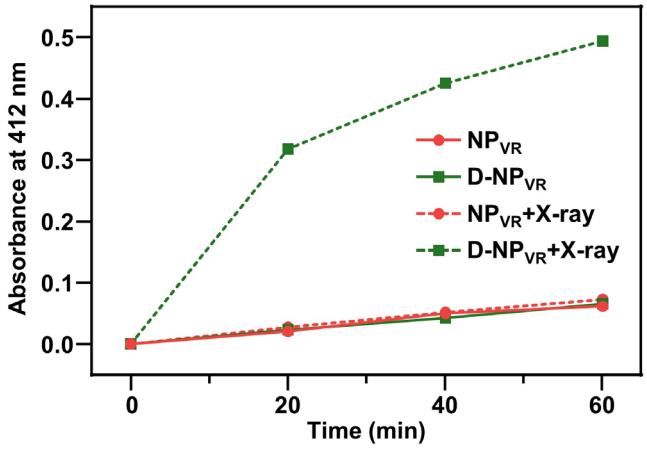


**Figure S5.** Bis(2-hydroxyethylthio)ethylene linker degradation of D-$NP_{VR}$ with or without 4 Gy of X-ray radiation.

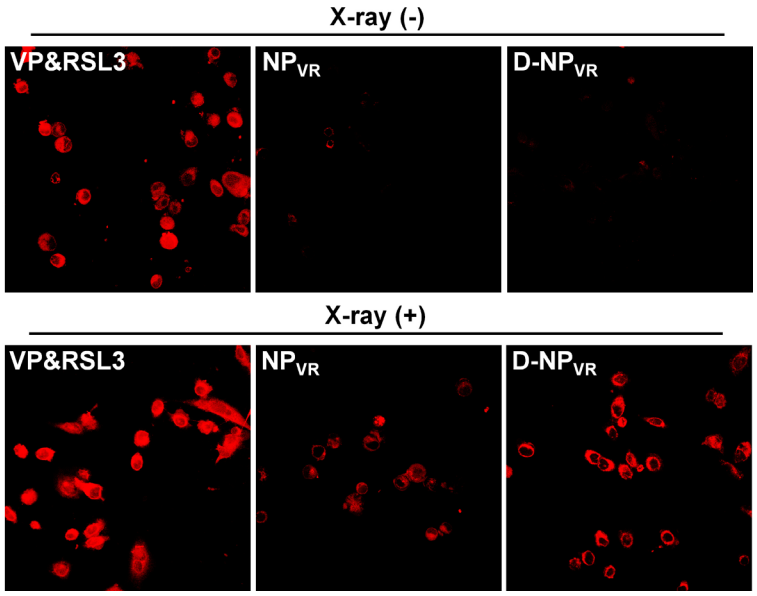


**Figure S6.** Fluorescent imaging of lipid peroxides in 4T1 cells. The cells were treated by various formulations including VP&RSL3, $NP_{VR}$, and D-$NP_{VR}$.

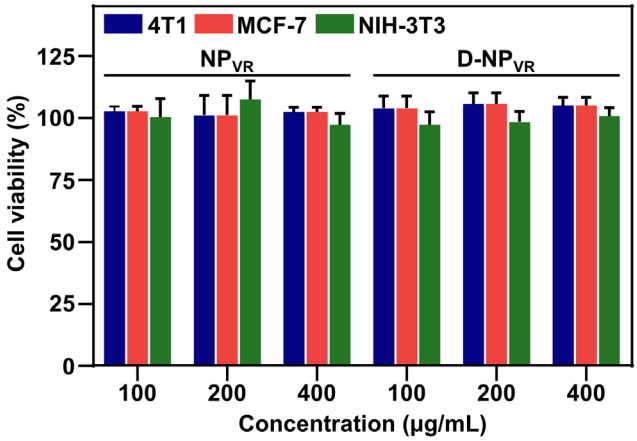


**Figure S7.** Relative viabilities after incubation with $NP_{VR}$ or D-$NP_{VR}$ on 4T1, MCF-7 and NIH-3T3 cells.

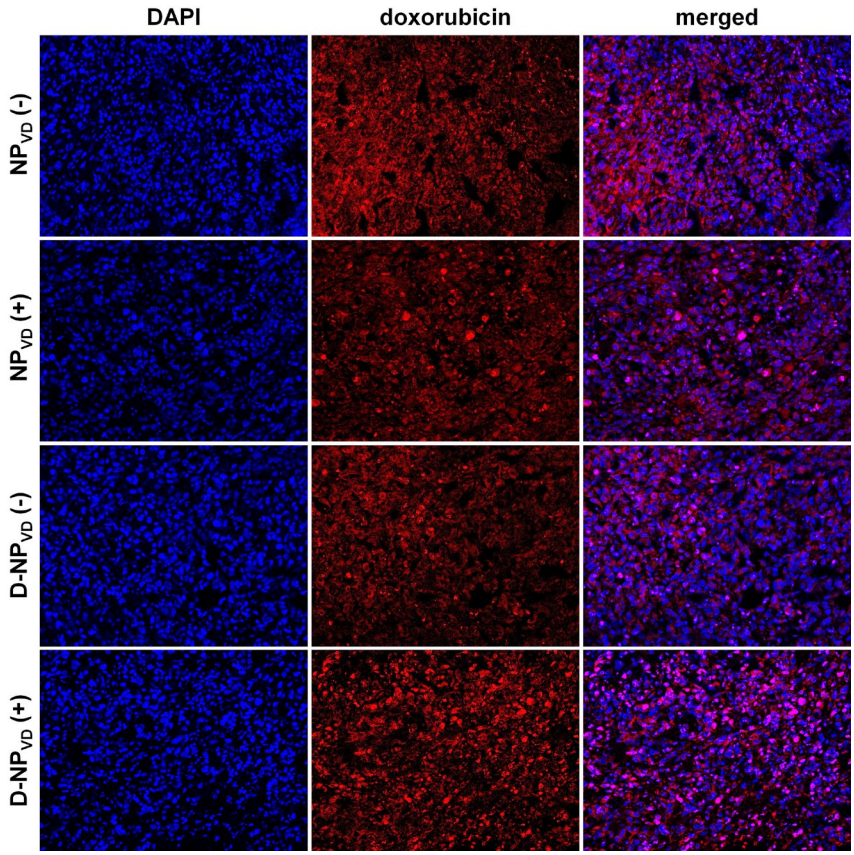


**Figure S8.** Following *i.v.* injections, the doxorubicin fluorescence observed by CLSM at 24 h with (+) or without (-) X-ray radiation.

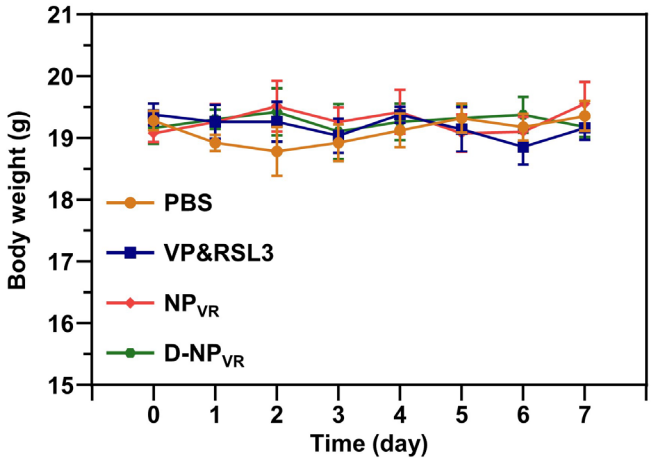


**Figure S9.** Body weight change following multiple *i.v.* injections of PBS, free VP&RSL3, $NP_{VR}$ or D-$NP_{VR}$.

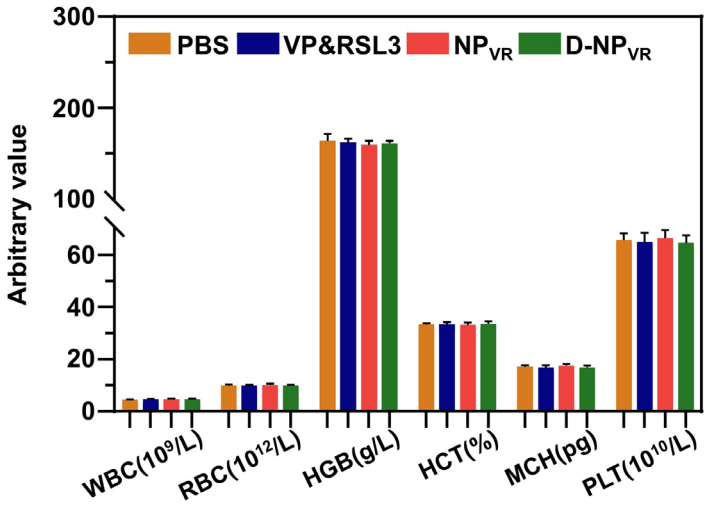


**Figure S10.** Complete blood count in BALB/c mice after *i.v.* injections (n = 5).

**Table S1.** Drug loading contents (DLC) and encapsulation efficiencies (EE) of VP and RSL3 for $NP_{VR}$ and D-$NP_{VR}$.

| | DLC (%) | | EE (%) | |
|---|---|---|---|---|
| | VP | RSL3 | VP | RSL3 |
| $NP_{VR}$ | 3.39 | 3.22 | 35.9 | 34.1 |
| D-$NP_{VR}$ | 3.53 | 3.07 | 34.6 | 30.1 |